4 Mobile Robot Vehicles

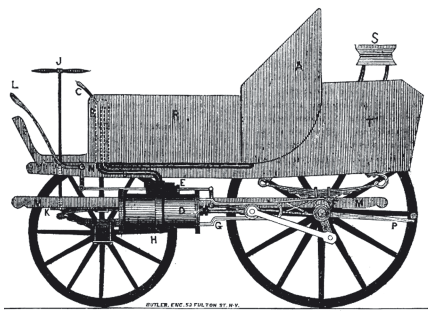

This chapter discusses how a robot platform moves, that is, how its pose changes with time as a function of its control inputs. There are many different types of robot platform as shown on pages 61–63 but in this chapter we will consider only two which are important exemplars. The first is a wheeled vehicle like a car which operates in a 2-dimensional world. It can be propelled forwards or backwards and its heading direction controlled by changing the angle of its steered wheels. The second platform is a quadrotor, a flying vehicle, which is an example of a robot that moves in 3-dimensional space. Quadrotors are becoming increasing popular as a robot platform since they can be quite easily modelled and controlled.

However before we start to discuss these two robot platforms it will be helpful to consider some general, but important, concepts regarding mobility.

4.1 Mobility

We have already touched on the diversity of mobile robots and their modes of locomotion. In this section we will discuss mobility which is concerned with how a vehicle moves in space.

We first consider the simple example of a train. The train moves along rails and its position is described by its distance along the rail from some datum. The *configuration* of the train can be completely described by a scalar parameter q which is called its generalized coordinate. The set of all possible configurations is the configuration space, or C-space, denoted by $\mathcal{C}$ and $q \in \mathcal{C}$. In this case $\mathcal{C} \subset \mathbb{R}$. We also say that the train has one degree of freedom since q is a scalar. The train also has one actuator (motor) that propels it forwards or backwards along the rail. With one motor and one degree of freedom the train is fully actuated and can achieve any desired configuration, that is, any position along the rail.

Another important concept is task space which is the set of all possible poses ξ of the vehicle and $\xi \in \mathcal{T}$. The task space depends on the application or task. If our task was motion along the rail then $\mathcal{T} \subset \mathbb{R}$. If we cared only about the position of the train in a plane then $\mathcal{T} \subset \mathbb{R}^2$. If we considered a 3-dimensional world then $\mathcal{T} \subset SE(3)$, and its height changes as it moves up and down hills and its orientation changes as it moves around curves. Clearly for these last two cases the dimensions of the task space exceed the dimensions of the configuration space and the train cannot attain an arbitrary pose since it is constrained to move along fixed rails. In these cases we say that the train moves along a manifold in the task space and there is a mapping from $q \mapsto \xi$.

Interestingly many vehicles share certain characteristics with trains – they are good at moving forward but not so good at moving sideways. Cars, hovercrafts, ships and aircraft all exhibit this characteristic and require complex manoeuvring in order to move sideways. Nevertheless this is a very sensible design approach since it caters to the motion we most commonly require of the vehicle. The less common motions such as parking a car, docking a ship or landing an aircraft are more complex, but not impossible, and humans can learn this skill. The benefit of this type of design comes from simplification and in particular reducing the number of actuators required.

Next consider a hovercraft which has two propellors whose axes are parallel but not collinear. The sum of their thrusts provide a forward force and the difference in thrusts generates a yawing torque for steering. The hovercraft moves over a planar surface and its configuration is entirely described by three generalized coordinates $\boldsymbol{q} = (x, y, \theta) \in \mathcal{C}$ and in this case $\mathcal{C} \subset \mathbb{R}^2 \times \mathbb{S}$. The configuration space has 3 dimensions and the vehicle therefore has three degrees of freedom.

The hovercraft has only two actuators, one fewer than it has degrees of freedom, and it is therefore an under-actuated system. This imposes limitations on the way in which it can move. At any point in time we can control the forward (parallel to the thrust vectors) acceleration and the rotational acceleration of the the hovercraft but there is zero sideways (or lateral) acceleration since it does not generate any lateral thrust. Nevertheless with some clever manoeuvring, like with a car, the hovercraft can follow a path that will take it to a place to one side of where it started. The advantage of under-actuation is the reduced number of actuators, in this case two instead of three. The penalty is that the vehicle cannot move directly to an any point in its configuration space, it must follow some path. If we added a third propellor to the hovercraft with its axis normal to the first two then it would be possible to command an arbitrary forward, sideways and rotational acceleration. The task space of the hovercraft is $\mathcal{T} \subset SE(2)$ which is equivalent, in this case, to the configuration space.

A helicopter has four actuators. The main rotor generates a thrust vector whose magnitude is controlled by the collective pitch, and the thrust vector's direction is controlled by the lateral and longitudinal cyclic pitch. The fourth actuator, the tail rotor, provides a yawing moment. The helicopter's configuration can be described by six generalized coordinates $\boldsymbol{q} = (x, y, z, \theta_r, \theta_p, \theta_y) \in \mathcal{C}$ which is its position and orientation in 3-dimensional space, with orientation expressed in roll-pitch-yaw angles. The configuration space $\mathcal{C} \subset \mathbb{R}^3 \times \mathbb{S}^3$ has six dimensions and therefore the vehicle has six degrees of freedom. The helicopter is under-actuated and it has no means to rotationally accelerate in the pitch and roll directions but cleverly these unactuated degrees of freedom are not required for helicopter operation – the helicopter naturally maintains stable equilibrium values for roll and pitch angle. Gravity acts like an additional actuator and provides a constant downward force. This allows the helicopter to accelerate sideways using the horizontal component of its thrust vector, while the vertical component of thrust is counteracted by gravity – without gravity a helicopter could not fly sideways. The task space of the helicopter is $\mathcal{T} \subset SE(3)$.

A fixed-wing aircraft moves forward very efficiently and also has four actuators (forward thrust, ailerons, elevator and rudder). The aircraft's thrust provides acceleration in the forward direction and the control surfaces exert various moments on the aircraft: rudder (yaw torque), ailerons (roll torque), elevator (pitch torque). The aircraft's configuration space is the same as the helicopter and has six dimensions. The aircraft is under-actuated and it has no way to accelerate in the lateral direction. The task space of the aircraft is $\mathcal{T} \subset SE(3)$.

Some low-cost hobby aircraft have no rudder and rely only on ailerons to bank and turn the aircraft. Even cheaper hobby aircraft have no elevator and rely on engine speed to control height.

The DEPTHX underwater robot shown on page 62 also has a configuration space $\mathcal{C} \subset \mathbb{R}^3 \times \mathbb{S}^3$ of six dimensions, but by contrast is fully actuated. Its six actuators can exert an arbitrary force and torque on the vehicle, allowing it to accelerate in any direction or about any axis. Its task space is $\mathcal{T} \subset SE(3)$.

Finally we come to the wheel – one of humanity's greatest achievements. The wheel was invented around 3000 BCE and the two wheeled cart was invented around 2000 BCE. Today four wheeled vehicles are ubiquitous and the total automobile population of the planet is approaching one billion. The effectiveness of cars, and our familiarity with them, makes them a natural choice for robot platforms that move across the ground.

http://hypertextbook.com/facts/2001/MarinaStasenko.shtml.

The configuration of a car moving over a plane is described by its generalized coordinates $\boldsymbol{q} = (x, y, \theta) \in \mathcal{C}$ and $\mathcal{C} \subset \mathbb{R}^2 \times \mathbb{S}$ which has 3 dimensions. A car has only two actuators, one to move forwards or backwards and one to change the heading direction. The car is therefore under-actuated. As we have already remarked an under-actuated vehicle cannot move directly to an any point in its configuration space, it

Unlike the aircraft and underwater robot the motion of a car is generally considered in terms of velocities rather than forces and torques.

Fig. 4.1. Omni-directional (or Swedish) wheel. Note the circumferential rollers which make motion in the direction of the wheel's axis almost frictionless. (Courtesy Vex Robotics)

must generally follow some nonlinear path. We know from our everyday experience with cars that it is not possible to drive sideways, but with some practice we can learn to follow a path that results in the vehicle being to one side of its initial position – this is parallel parking. Neither can a car rotate on spot, but we can follow a path that results in the vehicle being at the same position but rotated by 180° – a three-point turn. The challenges this introduces for control and path planning will be discussed in the rest of this part of the book. Despite this limitation the car is the simplest and most effective means of moving in a planar world that we have yet found.

The standard wheel is highly directional and prefers to roll in the direction normal to the axis of rotation. We might often wish for an ability to roll sideways but the standard wheel provides significant benefit when cornering – lateral friction between the wheels and the road counteracts, for free, the centripetal acceleration which would otherwise require an extra actuator to provide that force. More radical types of wheels have been developed that can roll sideways. An omni-directional wheel or Swedish wheel is shown in Fig. 4.1. It is similar to a normal wheel but has a number of passive rollers around its circumference and their rotational axes lie in the plane of the wheel. It is driven like an ordinary wheel but has very low friction in the lateral direction. A spherical wheel is similar to the roller ball in an old-fashioned computer mouse but driven by two actuators so that it can achieve achieve a velocity in any direction.

In robotics a car is often described as a non-holonomic vehicle. The term non-holonomic comes from mathematics and means that the motion of the car is subject to one or more non-holonomic constraints. A holonomic constraint is an equation that can be written in terms of the configuration variables x, y and θ. A non-holonomic constraint can only be written in terms of the *derivatives* of the configuration variables and *cannot be integrated* to a constraint in terms of configuration variables. Such systems are therefore also known as non-integrable systems. A key characteristic of these systems, as we have already discussed, is that they cannot move directly from one configuration to another – they must perform a manoeuvre or sequence of motions◂.

We can also consider this in control theoretic terms. Brockett's theorem (Brockett 1983) states that such systems are controllable but they cannot be stabilized to a desired state using a differentiable, or even continuous, pure state feedback controller. A time varying or non-linear control strategy is required.

A skid-steered vehicle, such as a tank, can turn on the spot but to move sideways it would have to stop, turn, proceed, stop then turn – this is a manoeuvre or time-varying control strategy which is the hallmark of a non-holonomic system. The tank has two actuators, one for each track, and just like a car is under-actuated.

Mobility parameters for the vehicles that we have discussed are tabulated in Table 4.1. The second column is the number of degrees of freedom of the vehicle or the dimension of its configuration space. The third column is the number of actuators and the fourth column indicates whether or not the vehicle is fully actuated.

4.2 Car-like Mobile Robots

Wheeled cars are a very effective class of vehicle and the archetype for most ground robots such as those shown on page 62. In this section we will create a model for a car-like vehicle and develop controllers that can drive the car to a point, along a line, follow an arbitrary path, and finally, drive to a specific pose.

Table 4.1. Summary of parameters for three different types of vehicle. The +g notation indicates that the gravity field can be considered as an extra actuator

Vehicle	Degrees of freedom	Number of actuators	Fully actuated?
Train	1	1	✓
Hovercraft	3	2	×
Helicopter	6	4+g	×
Fixed wing aircraft	6	4+g	×
6-thruster AUV	6	6	✓
Car	3	2	×

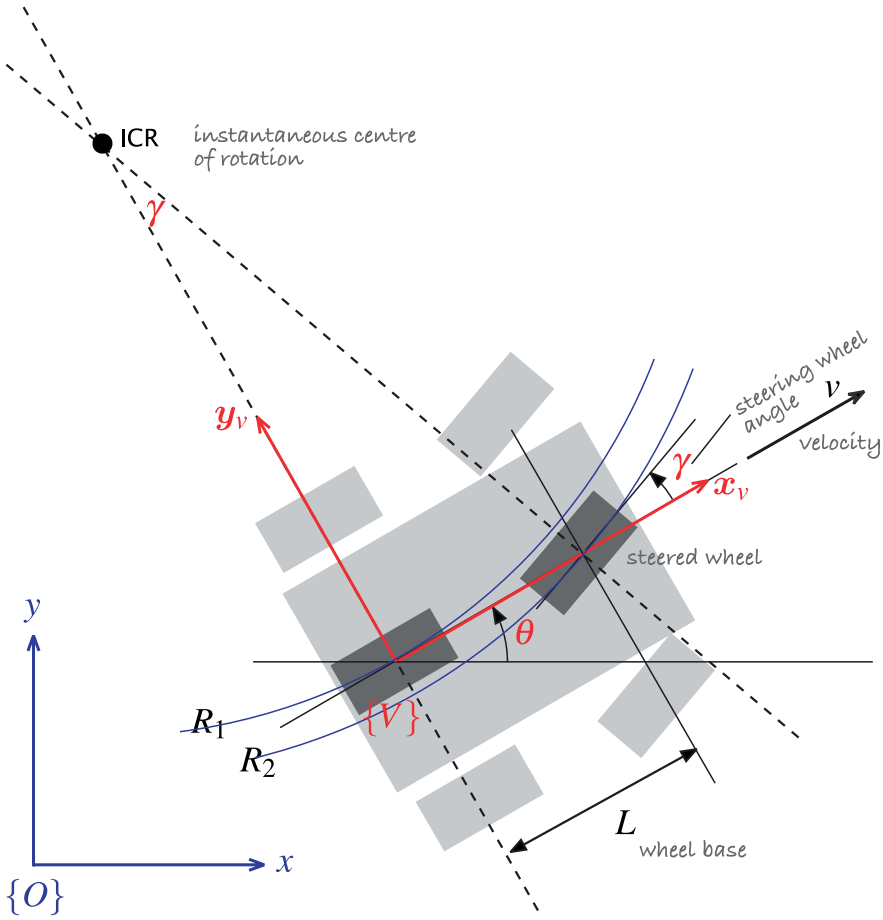

Fig. 4.2.
Bicycle model of a car. The car is shown in light grey, and the bicycle approximation is dark grey. The vehicle's coordinate frame is shown in red, and the world coordinate frame in blue. The steering wheel angle is γ and the velocity of the back wheel, in the x-direction, is v. The two wheel axes are extended as dashed lines and intersect at the Instantaneous Centre of Rotation (ICR) and the distance from the ICR to the back and front wheels is R_1 and R_2 respectively

A commonly used model for a four-wheeled car-like vehicle is the bicycle model shown in Fig. 4.2. The bicycle has a rear wheel fixed to the body and the plane of the front wheel rotates about the vertical axis to steer the vehicle.

Often incorrectly called the Ackerman model.

The pose of the vehicle is represented by the coordinate frame $\{V\}$ shown in Fig. 4.2, with its x-axis in the vehicle's forward direction and its origin at the centre of the rear axle. The configuration of the vehicle is represented by the generalized coordinates $\boldsymbol{q} = (x, y, \theta) \in \mathcal{C}$ where $\mathcal{C} \subset SE(2)$. The vehicle's velocity is by definition v in the vehicle's x-direction, and zero in the y-direction since the wheels cannot slip sideways. In the vehicle frame $\{V\}$ this is

Other well known models include the Reeds-Shepp model which has only three speeds: forward, backward and stopped, and the Dubbins car which has only two speeds: forward and stopped.

$$ {}^{V}\dot{x} = v, \quad {}^{V}\dot{y} = 0 $$

The dashed lines show the direction along which the wheels cannot move, the lines of no motion, and these intersect at a point known as the Instantaneous Centre of Rotation (ICR). The reference point of the vehicle thus follows a circular path and its angular velocity is

$$ \dot{\theta} = \frac{v}{R_1} \tag{4.1} $$

and by simple geometry the turning radius is $R_1 = L / \tan\gamma$ where L is the length of the vehicle or *wheel base*. As we would expect the turning circle increases with vehicle length. The steering angle γ is limited mechanically and its maximum value dictates the minimum value of R_1.

Vehicle coordinate system. The coordinate system that we will use, and a common one for vehicles of all sorts is that the x-axis is forward (longitudinal motion), the y-axis is to the left side (lateral motion) which implies that the z-axis is upward. For aerospace and underwater applications the z-axis is often downward and the x-axis is forward.

Paths that arcs with smoothly varying radius.

For a fixed steering wheel angle the car moves along a circular arc. For this reason curves on roads are circular arcs or clothoids◀ which makes life easier for the driver since constant or smoothly varying steering wheel angle allow the car to follow the road. Note that $R_2 > R_1$ which means the front wheel must follow a longer path and therefore rotate more quickly than the back wheel. When a four-wheeled vehicle goes around a corner the two steered wheels follow circular paths of different radius and therefore the angles of the steered wheels γ_L and γ_R should be very slightly different. This is achieved by the commonly used Ackerman steering mechanism which results in lower wear and tear on the tyres. The driven wheels must rotate at different speeds on corners which is why a differential gearbox is required between the motor and the driven wheels.

The velocity of the robot in the world frame is $(v\cos\theta, v\sin\theta)$ and combined with Eq. 4.1 we write the equations of motion as

$$\begin{aligned}\dot{x} &= v\cos\theta \\ \dot{y} &= v\sin\theta \\ \dot{\theta} &= \frac{v}{L}\tan\gamma\end{aligned} \tag{4.2}$$

This model is referred to as a kinematic model since it describes the velocities of the vehicle but not the forces or torques that cause the velocity. The rate of change of heading $\dot{\theta}$ is referred to as turn rate, heading rate or yaw rate and can be measured by a gyroscope. It can also be deduced from the angular velocity of the wheels on the left- and right-hand sides of the vehicle which follow arcs of different radius and therefore rotate at different speeds.

In the world coordinate frame we can write an expression for velocity in the vehicle's y-direction

$$\dot{y}\cos\theta - \dot{x}\sin\theta \equiv 0$$

which is the non-holonomic constraint. This equation cannot be integrated to form a relationship between x, y and θ.

Equation 4.2 captures some other important characteristics of a wheeled vehicle. When $v = 0$ then $\dot{\theta} = 0$, that is, it is not possible to change the vehicle's orientation when it is not moving. As we know from driving we must be moving in order to turn. If the steering angle is $\frac{\pi}{2}$ then the front wheel is orthogonal to the back wheel, the vehicle cannot move forward and the model enters an undefined region.

Rudolph Ackerman (1764–1834) was a German inventor born at Schneeberg, in Saxony. For financial reasons he was unable to attend university and became a saddler like his father. For a time he worked as a saddler and coach-builder and in 1795 established a print-shop and drawing-school in London. He published a popular magazine "The Repository of Arts, Literature, Commerce, Manufactures, Fashion and Politics" that included an eclectic mix of articles on water pumps, gas-lighting, and lithographic presses, along with fashion plates and furniture designs. He manufactured paper for landscape and miniature painters, patented a method for waterproofing cloth and paper and built a factory in Chelsea to produce it. He is buried in Kensal Green Cemetery, London.

In 1818 Ackermann took out British patent 4212 on behalf of the German inventor George Lankensperger for a steering mechanism which ensures that the steered wheels move on circles with a common centre. The same scheme was proposed and tested by Erasmus Darwin (grandfather of Charles) in the 1760s. Subsequent refinement by the Frenchman Charles Jeantaud led to the mechanism used in cars to this day which is known as Ackermann steering.

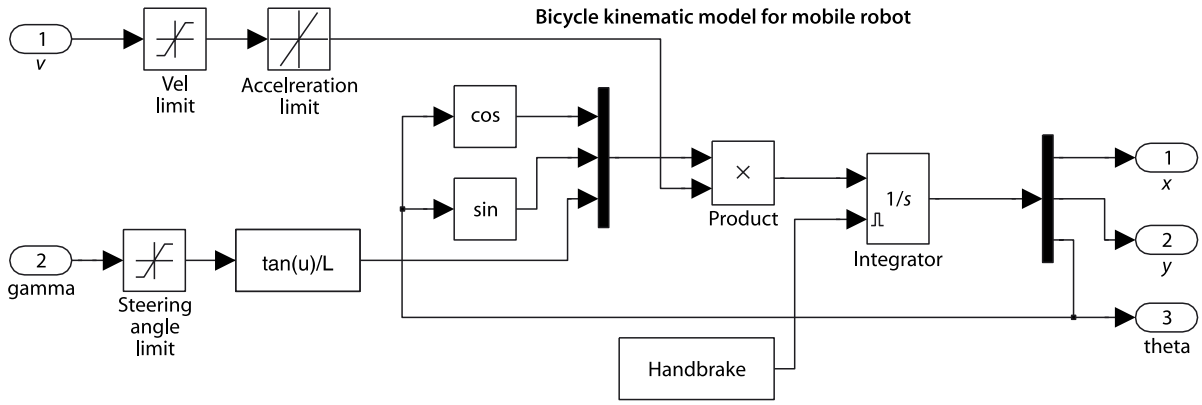

Fig. 4.3. Toolbox `Bicycle` block implements the bicycle kinematic model. The velocity input has a rate limiter to model finite acceleration, and limiters on velocity and steering wheel angle. The block labelled handbrake is a constant, from the block's parameter dialog, that resets the integrator and enforces the initial condition

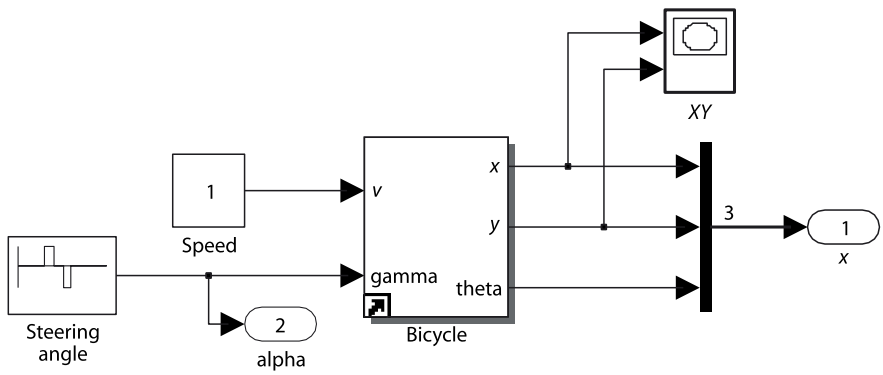

Fig. 4.4. Simulink® model `sl_lanechange` that results in a lane changing manoeuvre. The pulse generator drives the steering angle left then right

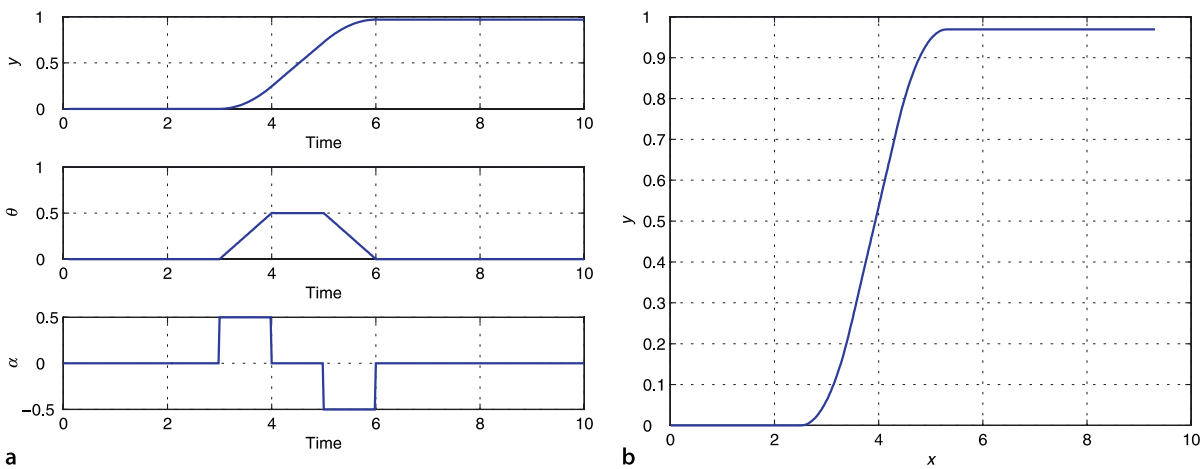

Fig. 4.5. Simple lane changing maneuver. **a** Vehicle response as a function of time, **b** motion in the *xy*-plane, the vehicle moves in the positive *x*-direction

Figure 4.3 shows a Simulink® implementation of the bicycle model. It implements Eq. 4.2 and also includes a maximum velocity limit, a velocity rate limiter to model finite acceleration and a limiter on the steering angle to model the finite range of the steered wheel. The Simulink® system

```
>> sl_lanechange
```

shown in Fig. 4.4 uses the `Bicycle` block in a system with a constant velocity demand. The steering input is a positive then negative pulse on the steering angle and the configuration is plotted against time in Fig. 4.5a. The result, in the *xy*-plane, is shown in Fig. 4.5b and shows a simple *lane-changing* trajectory.

4.2.1 Moving to a Point

Consider the problem of moving toward a goal point (x^*, y^*) in the plane. We will control the robot's velocity to be proportional to its distance from the goal

$$v^* = K_v \sqrt{(x^* - x)^2 + (y^* - y)^2}$$

and to steer toward the goal which is at the vehicle-relative angle in the world frame of

$$\theta^* = \tan^{-1} \frac{y^* - y}{x^* - x}$$

using a proportional controller

$$\gamma = K_h(\theta^* \ominus \theta), \quad K_h > 0$$

which turns the steering wheel toward the target. Note the use of the $\ominus$ operator since $\theta^*, \theta \in \mathbb{S}$ we require the angular difference◂ to also lie within $\mathbb{S}$. A Simulink® model

The Toolbox function `angdiff` computes the difference between two angles and returns a difference in the interval $[-\pi, \pi)$. Also available in the Toolbox Simulink® blockset `roblocks`.

```
>> sl_drivepoint
```

is shown in Fig. 4.6. We specify a goal coordinate

```
>> xg = [5 5];
```

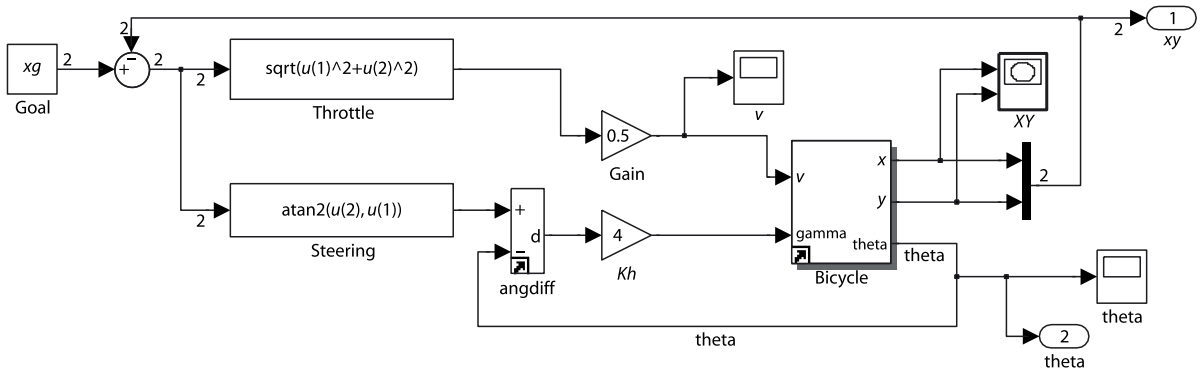

Fig. 4.6. `sl_drivepoint`, the Simulink® model that drives the vehicle to a point

To run the Simulink® model called `model` we first load it

```
>> model
```

and a new window is popped up that displays the model in block-diagram form. The simulation can be started by typing control-T or by using `Simulation+Start` option from the toolbar on the model's window. The model can also be run directly from the MATLAB® command line

```
>> sim('model')
```

Many Toolbox models create additional figures to display robot animations or graphs.

Some models write data to the MATLAB® workspace for subsequent analysis. Some models simply have unconnected output ports. All models in this chapter have the simulation data export option set to `Format=Array`, so the signals are concatenated, in port number order, to form a row vector and these are stacked to form a matrix `yout` with one row per timestep. The corresponding time values form a vector `tout`. These variables can be returned from the simulation

```
>> r = sim('model')
```

in the object `r`. Displaying `r` lists the variables that it contains and their value is obtained using the `find` method, for example

```
>> t = r.find('tout');
```

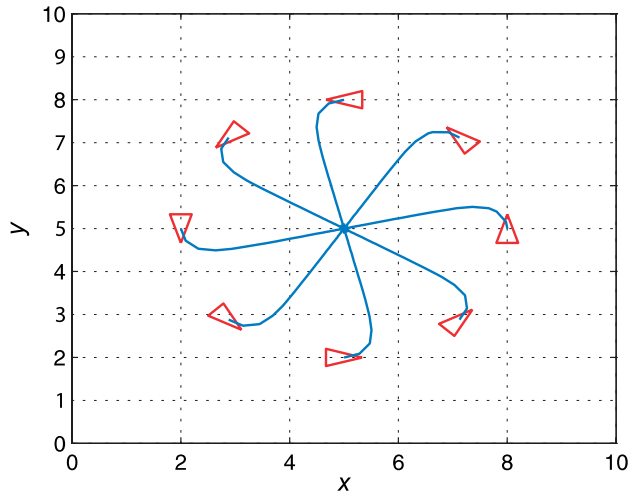

Fig. 4.7.
Simulation results for `sl_drivepoint` for different initial poses. The goal is (5, 5)

and an initial pose

```
>> x0 = [8 5 pi/2];
```

and then simulate the motion

```
>> r = sim('sl_drivepoint');
```

The variable `r` is an object that contains the simulation results from which we extract the configuration as a function of time

```
>> q = r.find('yout');
```

The vehicle's path in the plane is

```
>> plot(q(:,1), q(:,2));
```

which is shown in Fig. 4.7 for a number of starting poses. In each case the vehicle has moved forward and turned onto a path toward the goal point. The final part of each path is a straight line and the final orientation therefore depends on the starting point.

4.2.2 Following a Line

Another useful task for a mobile robot is to follow a line on the plane defined by $ax + by + c = 0$. This requires two controllers to adjust steering. One controller steers the robot to minimize the robot's normal distance from the line which according to Eq. I.1 is

$$d = \frac{(a, b, c) \cdot (x, y, 1)}{\sqrt{a^2 + b^2}}$$

The proportional controller

$$\alpha_d = -K_d d,\ K_d > 0$$

turns the robot toward the line. The second controller adjusts the heading angle, or orientation, of the vehicle to be parallel to the line

$$\theta^* = \tan^{-1} \frac{-a}{b}$$

using the proportional controller

$$\alpha_h = K_h(\theta^* \ominus \theta),\ K_h > 0$$

The combined control law

$$\gamma = -K_d d + K_h(\theta^* \ominus \theta)$$

turns the steering wheel so as to drive the robot toward the line and move along it.

The Simulink® model

```
>> sl_driveline
```

See Appendix I.

is shown in Fig. 4.8. We specify the target line as a 3-vector (a, b, c)

```
>> L = [1 -2 4];
```

and an initial pose

```
>> x0 = [8 5 pi/2];
```

and then simulate the motion

```
>> r = sim('sl_driveline');
```

The vehicle's path for a number of different starting poses is shown in Fig. 4.9.

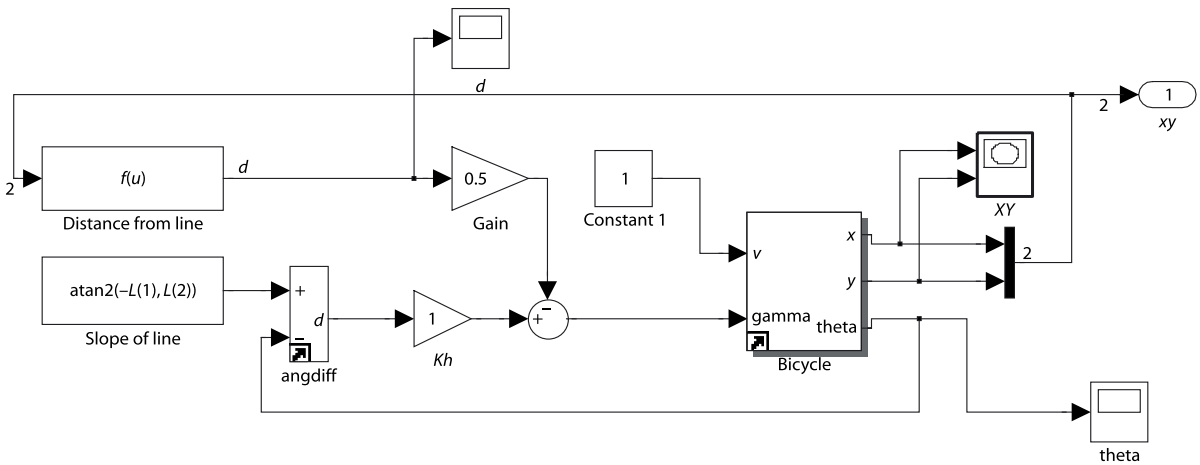

Fig. 4.8. The Simulink® model `sl_driveline` drives the vehicle along a line. The line parameters (a, b, c) are set in the workspace variable `L`

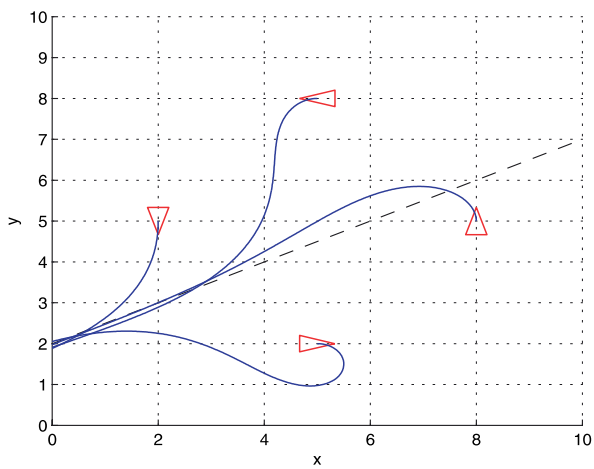

Fig. 4.9. Simulation results from different initial poses for the line $(1, -2, 4)$

4.2.3 Following a Path

Instead of a straight line we might wish to follow a path that is defined more generally as some locus on the *xy*-plane. The path might come from a sequence of coordinates generated by a motion planner, such as discussed in Sect. 5.2, or in real-time based on the robot's sensors.

A simple and effective algorithm for path following is pure pursuit in which the goal $(x^*(t), y^*(t))$ moves along the path, in its simplest form at constant speed, and the vehicle always heads toward the goal – think carrot and donkey.

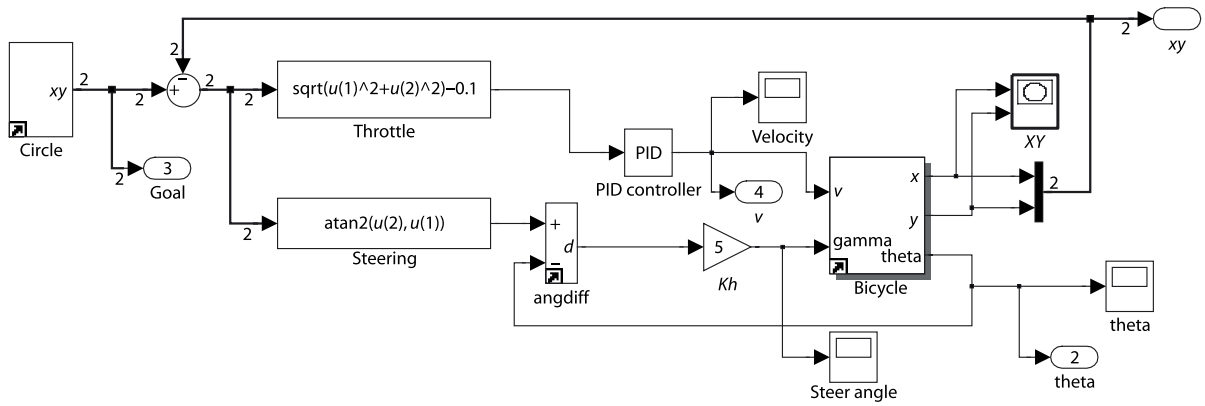

Fig. 4.10. The Simulink® model `sl_pursuit` drives the vehicle to follow an arbitrary moving target using pure pursuit. In this example the vehicle follows a point moving around a unit circle with a frequency of 0.1 Hz

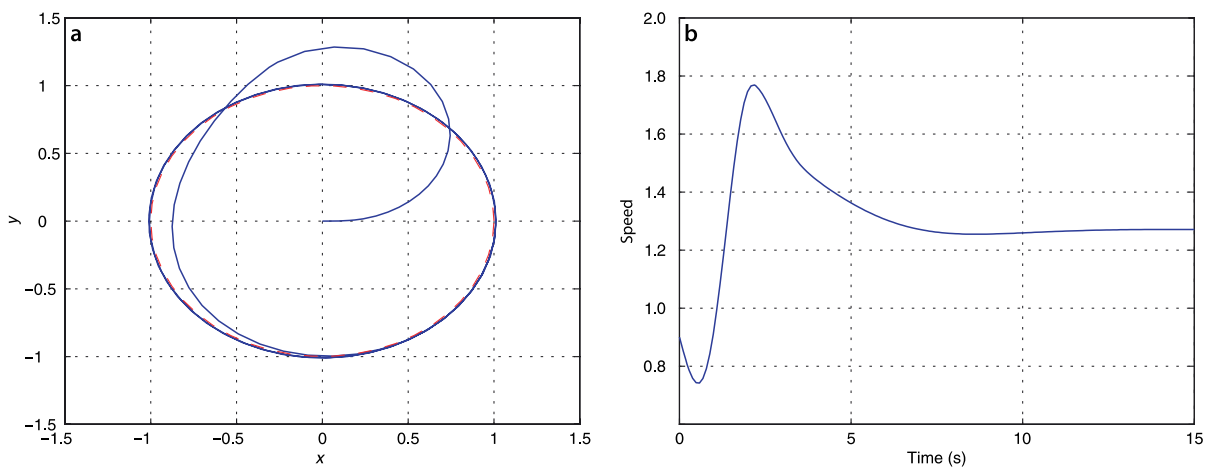

Fig. 4.11. Simulation results from pure pursuit. **a** Path of the robot in the *xy*-plane. The black dashed line is the circle to be tracked and the blue line in the path followed by the robot. **b** The speed of the vehicle versus time

This problem is very similar to the control problem we tackled in Sect. 4.2.1, moving to a point, except this time the point is moving. The robot maintains a distance d^* behind the pursuit point and we formulate an error

$$e = \sqrt{(x^* - x)^2 + (y^* - y)^2} - d^*$$

that we regulate to zero by controlling the robot's velocity using a proportional-integral (PI) controller

$$v^* = K_v e + K_i \int e \, dt$$

The integral term is required to provide a finite velocity demand v^* when the following error is zero. The second controller steers the robot toward the target which is at the relative angle

$$\theta^* = \tan^{-1} \frac{y^* - y}{x^* - x}$$

and a simple proportional controller

$$\alpha = K_h(\theta^* \ominus \theta), \quad K_h > 0$$

turns the steering wheel so as to drive the robot toward the target.

The Simulink® model

```
>> sl_pursuit
```

shown in Fig. 4.10 includes a target that moves around a unit circle. It can be simulated

```
>> r = sim('sl_pursuit')
```

and the results are shown in Fig. 4.11a. The robot starts at the origin but catches up to, and follows, the moving goal. Figure 4.11b shows how the speed demand picks up smoothly and converges to a steady state value at the desired following distance.

4.2.4 Moving to a Pose

The final control problem we discuss is driving to a specific pose (x^*, y^*, θ^*). The controller of Fig. 4.6 could drive the robot to a goal position but the final orientation depended on the starting position.

In order to control the final orientation we first rewrite Eq. 4.2 in matrix form

$$\begin{pmatrix} \dot{x} \\ \dot{y} \\ \dot{\theta} \end{pmatrix} = \begin{pmatrix} \cos\theta & 0 \\ \sin\theta & 0 \\ 0 & 1 \end{pmatrix} \begin{pmatrix} v \\ \gamma \end{pmatrix}$$

and then transform the equations into polar coordinate form using the notation shown in Fig. 4.12. We apply a change of variables

$$\rho = \sqrt{\Delta_x^2 + \Delta_y^2}$$

$$\alpha = \tan^{-1} \frac{\Delta_y}{\Delta_x} - \theta$$

$$\beta = -\theta - \alpha$$

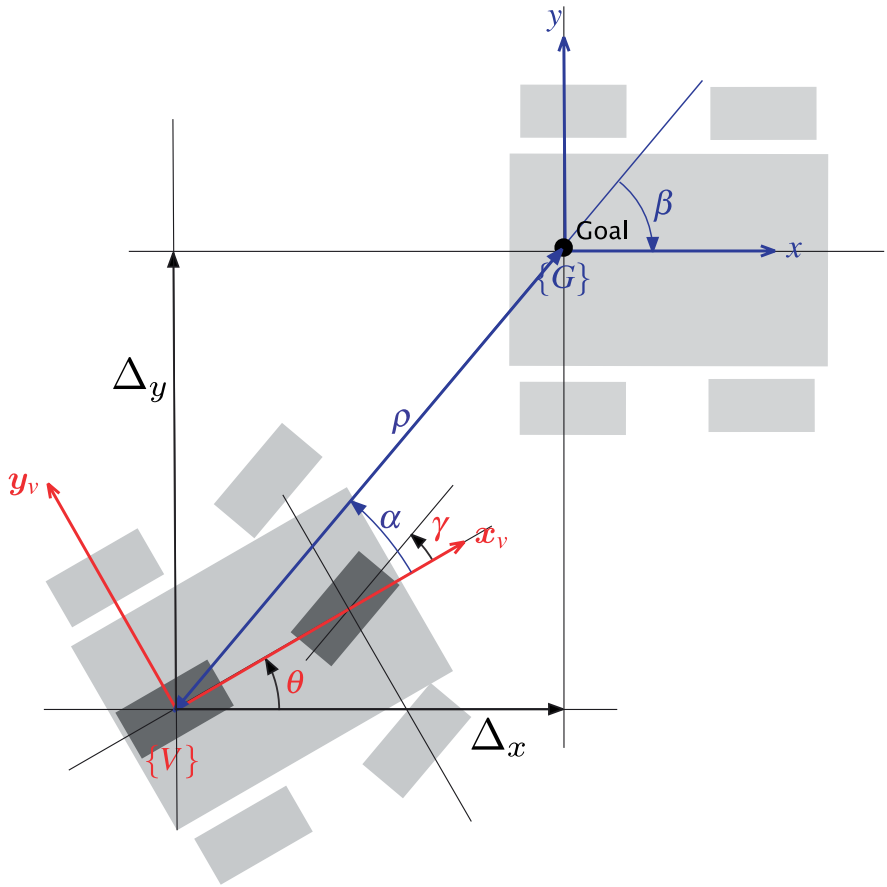

Fig. 4.12.
Polar coordinate notation for the bicycle model vehicle moving toward a goal pose: ρ is the distance to the goal, β is the angle of the goal vector with respect to the world frame, and α is the angle of the goal vector with respect to the vehicle frame

which results in

$$\begin{pmatrix}\dot{\rho}\\ \dot{\alpha}\\ \dot{\beta}\end{pmatrix} = \begin{pmatrix}-\cos\alpha & 0\\ \frac{\sin\alpha}{\rho} & -1\\ -\frac{\sin\alpha}{\rho} & 0\end{pmatrix}\begin{pmatrix}v\\ \gamma\end{pmatrix}, \quad \text{if } \alpha \in \left(-\frac{\pi}{2}, \frac{\pi}{2}\right]$$

and assumes the goal $\{G\}$ is in front of the vehicle. The linear control law

$$v = k_\rho \rho$$
$$\gamma = k_\alpha \alpha + k_\beta \beta$$

drives the robot to a unique equilibrium▸ at $(\rho, \alpha, \beta) = (0, 0, 0)$. The intuition behind this controller is that the terms $k_\rho\rho$ and $k_\alpha\alpha$ drive the robot along a line toward $\{G\}$ while the term $k_\beta\beta$ rotates the line so that $\beta \to 0$. The closed-loop system

The control law introduces a discontinuity at $\rho = 0$ which satisfies Brockett's theorem.

$$\begin{pmatrix}\dot{\rho}\\ \dot{\alpha}\\ \dot{\beta}\end{pmatrix} = \begin{pmatrix}-k_\rho \cos\alpha\\ k_\rho \sin\alpha - k_\alpha\alpha - k_\beta\beta\\ -k_\rho \sin\alpha\end{pmatrix}$$

is stable so long as

$$k_\rho > 0,\ k_\beta < 0,\ k_\alpha - k_\rho > 0$$

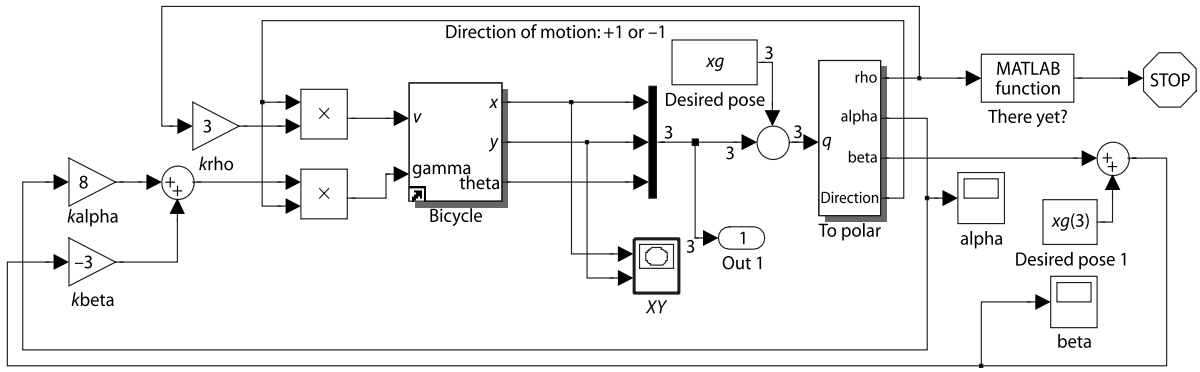

Fig. 4.13. The Simulink® model `sl_drivepose` drives the vehicle to a pose. The initial and final poses are set by the workspace variable `x0` and `xf` respectively

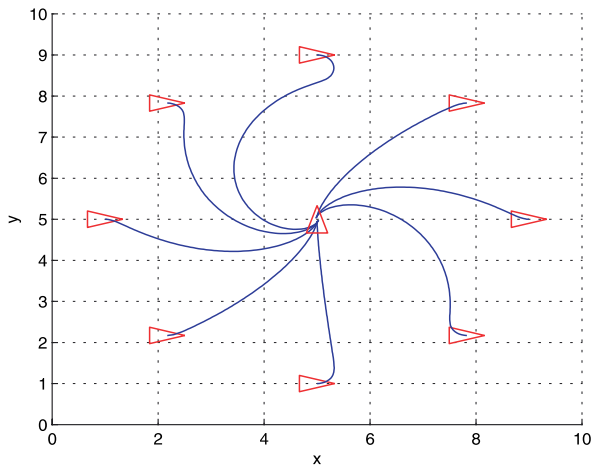

Fig. 4.14. Simulation results from different initial poses to the final pose $(5, 5, \frac{\pi}{2})$. Note that in some cases the robot has *backed into* the final pose

The distance and bearing to the goal (ρ, α) could be measured by a camera or laser range finder, and the angle β derived from α and vehicle orientation θ as measured by a compass.

For the case where the goal is behind the robot, that is $\alpha \notin (-\frac{\pi}{2}, \frac{\pi}{2}]$, we reverse the vehicle by negating v and γ in the control law. The velocity v always has a constant sign which depends on the initial value of α.

So far we have described a *regulator* that drives the vehicle to the pose (0, 0, 0). To move the robot to an arbitrary pose (x^*, y^*, θ^*) we perform a change of coordinates

$$x' = x - x^*,\ y' = y - y^*,\ \theta' = \theta,\ \beta = \beta' + \theta^*$$

The pose controller is implemented by the Simulink® model

```
>> sl_drivepose
```

shown in Fig. 4.13. We specify a goal pose

```
>> xg = [5 5 pi/2];
```

and an initial pose

```
>> x0 = [8 5 pi/2];
```

and then simulate the motion

```
>> r = sim('sl_drivepose');
```

As before, the simulation results are stored in `r` and can be plotted

```
>> y = r.find('yout');
>> plot(y(:,1), y(:,2));
```

to show the vehicle's path in the plane. The vehicle's path for a number of starting poses is shown in Fig. 4.14. The vehicle moves forwards or backward and takes a smooth path to the goal pose.▸

The controller is based on the linear bicycle model but the Simulink® model `Bicycle` has hard non-linearities including steering angle limits and velocity rate limiting.

4.3 Flying Robots

In order to fly, all one must do is simply miss the ground.
Douglas Adams

Flying robots or unmanned aerial vehicles (UAV) are becoming increasingly common and span a huge range of size and shape as shown in shown in Fig. 4.15. Applications include military operations, surveillance, meteorological investigations and robotics research. Fixed wing UAVs are similar in principle to passenger aircraft with wings to provide lift, a propellor or jet to provide forward thrust and control surface for manoeuvring. Rotorcraft UAVs have a variety of configurations that include conventional helicopter design with a main and tail rotor, a *coax* with counter-rotating coaxial rotors and quadrotors. Rotorcraft UAVs are used for inspection and research and have the advantage of being able to take off vertically.

Flying robots differ from ground robots in some important ways. Firstly they have 6 degrees of freedom and their configuration $\boldsymbol{q} \in SE(3)$. Secondly they are actuated by forces, that is their motion model is expressed in terms of forces and torques rather than velocities as was the case for the bicycle model – we use a dynamic rather than a kinematic model. Underwater robots have many similarities to flying robots and can be considered as vehicles that *fly through water* and there are underwater equivalents to fixed wing aircraft and rotorcraft. The principle differences underwater are an upward buoyancy force, drag forces that are much more significant than in air, and added mass.

In this section we will create a model for a quadrotor flying vehicle such as shown in Fig. 4.15d. Quadrotors are now widely available, both as commercial products and

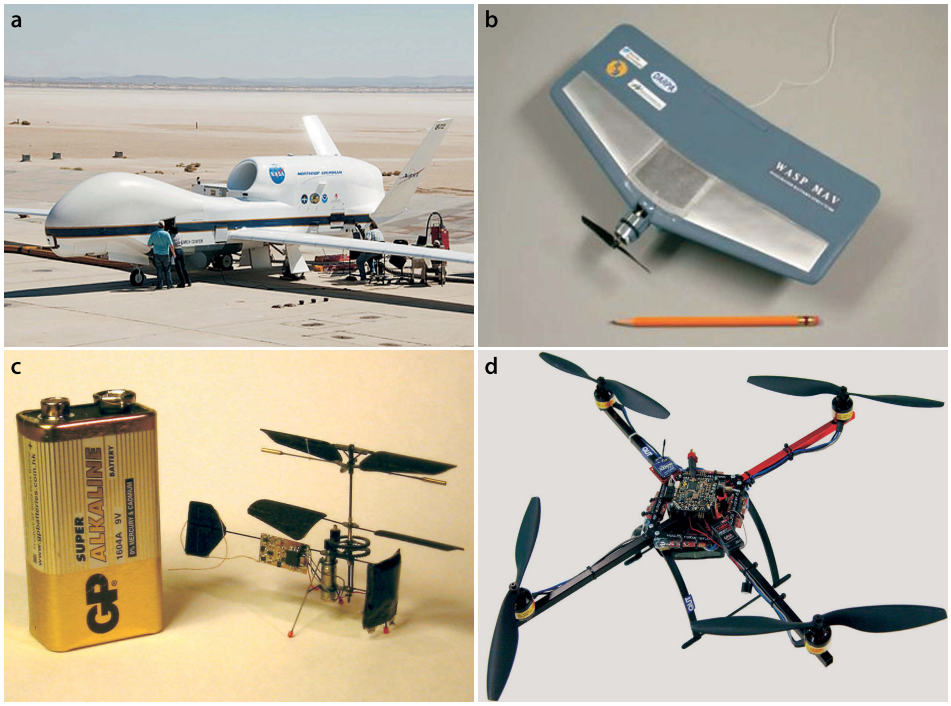

Fig. 4.15.
Flying robots. **a** Global Hawk unmanned aerial vehicle (UAV) (photo: courtesy of NASA), **b** a micro air vehicle (MAV) (photo: courtesy of AeroVironment, Inc.), **c** a 1 gram co-axial helicopter with 70 mm rotor diameter (photo courtesy of Petter Muren and Proxflyer AS), **d** a quadrotor, also known as an X4, which has four rotors and a block of sensing and control electronics are in the middle (photo: courtesy of Inkyu Sa)

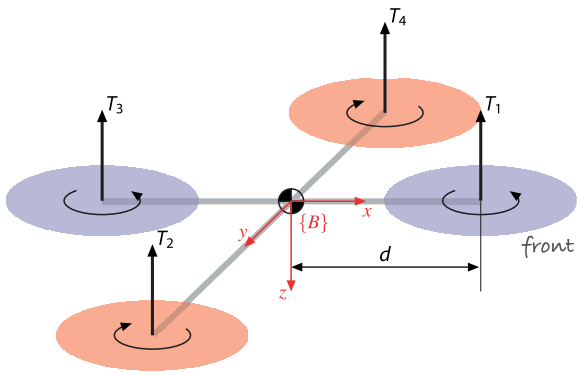

Fig. 4.16. Quadrotor notation showing the four rotors, their thrust vectors and directions of rotation. The body-fixed frame {*B*} is attached to the vehicle and has its origin at the vehicle's centre of mass. Rotors 1 and 3 rotate counter-clockwise (viewed from above) while rotors 2 and 4 rotate clockwise

as open-source projects. Compared to fixed wing aircraft they are highly manoeuvrable and can be flown safely indoors which makes them well suited for laboratory or hobbyist use. Compared to conventional helicopters, with the large main rotor and tail rotor, the quadrotor is easier to fly, does not have the complex swash plate mechanism and is easier to model and control.

The notation for the quadrotor model is shown in Fig. 4.16. The body-fixed coordinate frame {*B*} has its *z*-axis downward following the aerospace convention. The quadrotor has four rotors, labelled 1 to 4, mounted at the end of each cross arm. The rotors are driven by electric motors powered by electronic speed controllers. Some low-cost quadrotors use small motors and reduction gearing to achieve sufficient torque. The rotor speed is ω_i and the thrust is an upward vector

$$T_i = b\omega_i^2, \quad i = 1, 2, 3, 4 \tag{4.3}$$

in the vehicle's negative *z*-direction, where $b > 0$ is the lift constant that depends on the air density, the cube of the rotor blade radius, the number of blades, and the chord length of the blade.

The translational dynamics of the vehicle in world coordinates is given by Newton's second law

$$m\dot{\boldsymbol{v}} = \begin{pmatrix} 0 \\ 0 \\ mg \end{pmatrix} - {}^0\boldsymbol{R}_B \begin{pmatrix} 0 \\ 0 \\ T \end{pmatrix} \tag{4.4}$$

where $\boldsymbol{v}$ is the velocity of the vehicle in the world frame, g is gravitational acceleration, m is the total mass of the vehicle and $T = \Sigma T_i$ is the total upward thrust. The first term is the force of gravity which acts downward in the world frame and the second term is the total thrust in the vehicle frame rotated into the world coordinate frame.

Pairwise differences in rotor thrusts cause the vehicle to rotate. The torque about the vehicle's *x*-axis, the *rolling* torque, is

$$\tau_x = dT_4 - dT_2$$

where d is the distance from the motor to the centre of mass. We can write this in terms of rotor speeds by substituting Eq. 4.3

$$\tau_x = db\left(\omega_4^2 - \omega_2^2\right) \tag{4.5}$$

and similarly for the *y*-axis, the *pitching* torque is

$$\tau_y = db\left(\omega_1^2 - \omega_3^2\right) \tag{4.6}$$

The torque applied to each propellor by the motor is opposed by aerodynamic drag

$$Q_i = k\omega_i^2$$

where k depends on the same factors as b. This torque exerts a reaction torque on the airframe which acts to rotate the airframe about the propeller shaft in the opposite direction to its rotation. The total reaction torque about the z-axis is

$$\begin{aligned}\tau_z &= Q_1 - Q_2 + Q_3 - Q_4 \\ &= k\left(\omega_1^2 + \omega_3^2 - \omega_2^2 - \omega_4^2\right)\end{aligned} \tag{4.7}$$

where the different signs are due to the different rotation directions of the rotors. A yaw torque can be created simply by appropriate coordinated control of all four rotor speeds.

The rotational acceleration of the airframe is given by Euler's equation of motion

$$\boldsymbol{J}\dot{\omega} = -\omega \times \boldsymbol{J}\omega + \boldsymbol{\Gamma} \tag{4.8}$$

where $\boldsymbol{J}$ is the 3×3 inertia matrix of the vehicle, ω is the angular velocity vector and $\boldsymbol{\Gamma} = (\tau_x, \tau_y, \tau_z)^T$ is the torque applied to the airframe according to Eq. 4.5 to 4.7.

The motion of the quadrotor is obtained by integrating the forward dynamics equations Eq. 4.4 and Eq. 4.8 where the forces and moments on the airframe

$$\begin{pmatrix} T \\ \boldsymbol{\Gamma} \end{pmatrix} = \begin{pmatrix} -b & -b & -b & -b \\ 0 & -db & 0 & db \\ db & 0 & -db & 0 \\ k & -k & k & -k \end{pmatrix} \begin{pmatrix} \omega_1^2 \\ \omega_2^2 \\ \omega_3^2 \\ \omega_4^2 \end{pmatrix} = \boldsymbol{A} \begin{pmatrix} \omega_1^2 \\ \omega_2^2 \\ \omega_3^2 \\ \omega_4^2 \end{pmatrix} \tag{4.9}$$

are functions of the rotor speeds. The matrix $\boldsymbol{A}$ is of full rank if $b, k, d > 0$ and can be inverted

$$\begin{pmatrix} \omega_1^2 \\ \omega_2^2 \\ \omega_3^2 \\ \omega_4^2 \end{pmatrix} = \boldsymbol{A}^{-1} \begin{pmatrix} T \\ \tau_x \\ \tau_y \\ \tau_z \end{pmatrix} \tag{4.10}$$

to give the rotor speeds required to apply a specified thrust T and moment $\boldsymbol{\Gamma}$ to the airframe.

The rotational dynamics has a second-order transfer function of $\Theta_y(s)/\tau_y(s) = 1/(Js^2 + Bs)$ where B is aerodynamic damping which is generally quite small. To regulate a second-order system requires a proportional-derivative controller.

To control the vehicle we will employ a nested control structure which we illustrate for pitch and x-translational motion. The innermost loop uses a proportional and derivative controller to compute the required pitching torque on the airframe

$$\tau_y = K_p(\theta_p^* - \theta_p) + K_d(\dot{\theta}_p^* - \dot{\theta}_p)$$

The term $\dot{\theta}_p^*$ is commonly ignored.

based on the error between desired and actual pitch angle. The gains $K_{\tau,p}$ and $K_{\tau,d}$ are determined by classical control design approaches based on an approximate dynamic model and then tuned to achieve good performance. The actual vehicle pitch angle θ_p would be estimated by an inertial navigation system. The required rotor speeds are then determined using Eq. 4.10.

Consider a coordinate frame $\{V\}$ attached to the vehicle and with the same origin as $\{B\}$ but with its x- and y-axes parallel to the ground. To move the vehicle in the ^{V}x-direction we pitch the nose down which generates a force

$$\boldsymbol{f} = \boldsymbol{R}_y(\theta_p) \begin{pmatrix} 0 \\ 0 \\ T \end{pmatrix} = \begin{pmatrix} T\sin\theta_p \\ 0 \\ T\cos\theta_p \end{pmatrix}$$

which has a component

$$f_x = T \sin\theta_p \approx T\theta_p$$

that accelerates the vehicle in the ${}^{V}x$-direction. We can control the velocity in this direction with a proportional control law

$$f_x^* = mK_f\left({}^{V}v_x^* - {}^{V}v_x\right)$$

Combine these two equations we obtain the pitch angle

$$\theta_p^* = \frac{m}{T}K_f\left({}^{V}v_x^* - {}^{V}v_x\right) \tag{4.11}$$

required to achieve the desired forward velocity. The actual vehicle velocity ${}^{V}v_x$ would be estimated by an inertial navigation system or GPS receiver. For a vehicle in vertical equilibrium the total thrust equals the weight force so $m / T \approx 1 / g$.

If the position of the vehicle in the xy-plane of the world frame is $\boldsymbol{p} \in \mathbb{R}^2$ then the desired velocity is given by the proportional control law

$$\boldsymbol{v}^* = K_p(\boldsymbol{p}^* - \boldsymbol{p}) \tag{4.12}$$

based on the error between the desired and actual position. The desired velocity in frame $\{V\}$ is

$${}^{V}\boldsymbol{v} = {}^{V}\boldsymbol{R}_0(\theta_y)\boldsymbol{v} = {}^{0}\boldsymbol{R}_V^T(\theta_y)\boldsymbol{v}$$

which is a function of the yaw angle θ_y

$$\begin{pmatrix} {}^{V}v_x \\ {}^{V}v_y \end{pmatrix} = {}^{0}R_V^T(\theta_y)\begin{pmatrix} v_x \\ v_y \end{pmatrix}$$

To reach a desired position we can compute the appropriate velocity and from that the appropriate pitch angle which generates a force to move the vehicle. This indirection is a consequence of the vehicle being underactuated – we have just four rotor speeds to adjust but the vehicle's configuration space is 6-dimensional. To move forward the quadrotor airframe must first pitch down so that the thrust vector has a horizontal component to accelerate it.◀ As it approaches its goal the airframe must be rotated in the opposite direction, pitching up, so that the backward component of thrust decelerates the forward motion. Finally the airframe rotates to the horizontal with the thrust vector vertical. The cost of under-actuation is once again a manoeuvre. The pitch angle cannot be arbitrarily set, it is a means to achieve translation control.

The total thrust must be increased so that the vertical thrust component still balances gravity.

The rotational inertia of a body that moves in $SE(3)$ is represented by the 3×3 symmetric matrix

$$\boldsymbol{J} = \begin{pmatrix} J_{xx} & J_{xy} & J_{xz} \\ J_{xy} & J_{yy} & J_{yz} \\ J_{xz} & J_{yz} & J_{zz} \end{pmatrix}$$

The diagonal elements are the moments of inertia, and the off-diagonal elements are products of inertia. Only six of these nine elements are unique: three moments and three products of inertia. The products of inertia are zero if the object's mass distribution is symmetrical with respect to the coordinate frame.

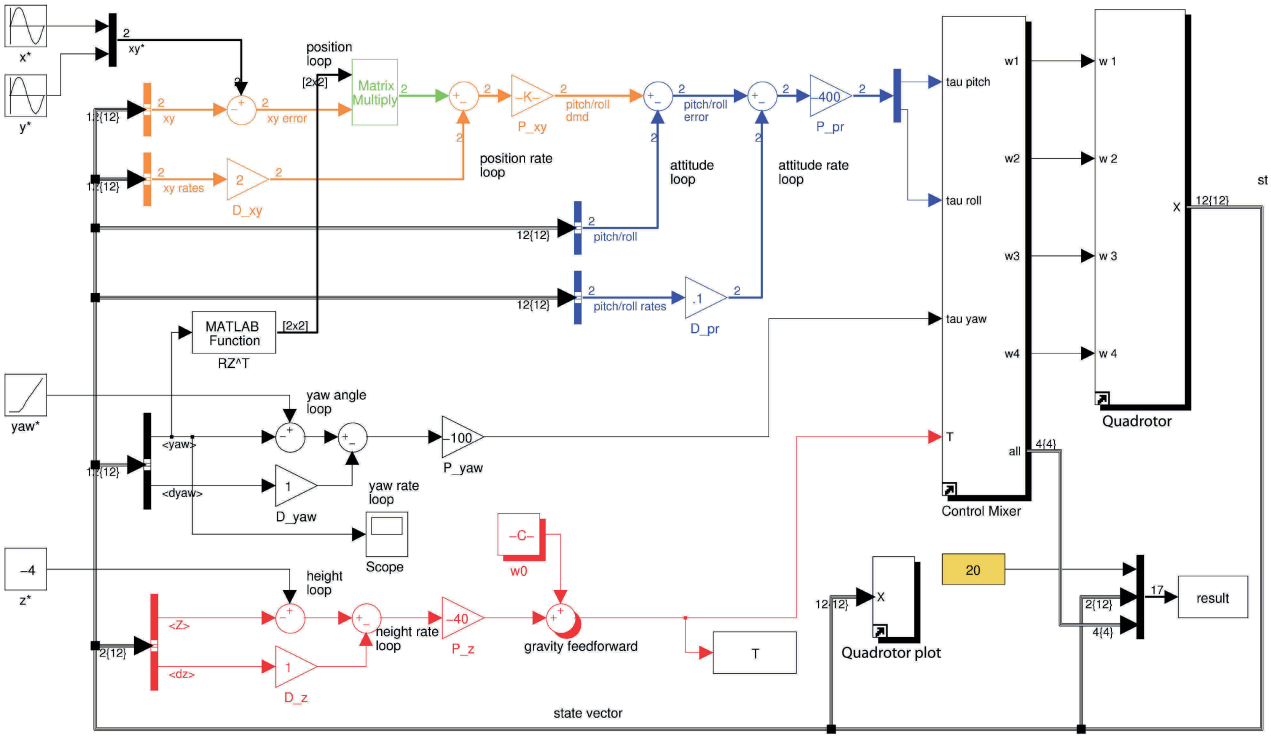

Fig. 4.17. The Simulink® model `sl_quadrotor` which is a closed-loop simulation of the quadrotor. The flyer takes off and flies in a circle at constant altitude. The dynamics block implements Eq. 4.9, and the mixer block implements its inverse while also enforcing limits on rotor speed. A Simulink® bus is used for the 12-element state vector `X` output by the `Quadrotor` block

Figure 4.17 shows a Simulink® model of the quadrotor in a closed-loop control structure. The inputs to the quadrotor block are the speeds of the four rotors and from Eq. 4.9 the torques and forces on the quadrotor are computed and it integrates Eq. 4.4, Eq. 4.8 and Eq. 4.9 to give the position, velocity, orientation and orientation rate. The output of this block is the state vector $\boldsymbol{x} = (x, y, z, \theta_r, \theta_p, \theta_y, \dot{x}, \dot{y}, \dot{z}, \dot{\theta}_r, \dot{\theta}_p, \dot{\theta}_y)$. As is common in aerospace applications we represent orientation and orientation rate in terms of roll-pitch-yaw angles. The control part of the block diagram involves multiple nested control loops that compute the required thrust and torques so that the vehicle moves to the setpoint.

The vehicle's position control loops, as just discussed, are shown in the top left of the diagram. The innermost loop, shown in blue, controls the attitude of the vehicle and its inputs are the actual and desired roll and pitch angles, as well as the roll and pitch angular rates to provide damping. The outer loop, shown in orange, controls the xy-position of the flyer by requesting changes in roll and pitch angle so as to provide a component of thrust in the direction of desired xy-plane motion. In the diagram Eq. 4.11 and Eq. 4.12 have been combined into the form

$$\theta_p^* = K_1\left({}^V p_x^* - {}^V p_x - K_2\, {}^V v_x\right)$$

The xy-position error is computed in the world frame and rotated by ${}^0\boldsymbol{R}_V^T(\theta_y)$ into frame $\{V\}$. Note that according to the coordinate conventions shown in Fig. 4.16 ${}^V x$-direction motion requires a negative rotation about the y-axis (pitch angle) and ${}^V y$-direction motion requires a positive rotation about the x-axis (roll angle) so the gains have different signs for the roll and pitch loops.

Yaw is controlled by a proportional-derivative controller

$$\tau_z = K_p\left(\theta_y^* - \theta_y\right) + K_d\left(\dot{\theta}_y^* - \dot{\theta}_y\right)$$

shown in black and $\dot{\theta}_y^*$ is ignored since it is typically small.

Altitude is controlled by a proportional-derivative controller

$$T = K_p(z^* - z) + K_d(\dot{z}^* - \dot{z}) + \omega_0$$

shown in red which which determines the average rotor speed. The additive term

$$\omega_0 = \sqrt{\frac{mg}{4b}} \tag{4.13}$$

is the rotor speed necessary to generate a thrust equal to the weight of the vehicle. This is an example of feedforward control – used here to counter the effect of gravity which otherwise is a constant disturbance to the altitude control loop. The alternatives to feedforward control would be to have very high gain for the altitude loop which often leads to actuator saturation and instability, or a proportional-integral (PI) controller which might require a long time for the integral term to increase to a useful value and then lead to overshoot. We will revisit gravity compensation in Chap. 9 applied to arm-type robots.

The parameters of a specific quadrotor can be loaded

```
>> mdl_quadrotor
```

which creates a structure called `quad` in the workspace, and its elements are the various dynamic properties of the quadrotor. The simulation can be run using the Simulink® menu or from the MATLAB® command line

```
>> sim('sl_quadrotor');
```

The simulation loads the default quadrotor model before it starts, through the `PreLoadFcn` callback set from model's properties File+Model Properties+Callbacks+PreLoadFcn.

and it displays an animation in a separate window. The vehicles lifts off and flies in a circle while spinning slowly about its own z-axis. A snapshot is shown in Fig. 4.18. The simulation writes the results from each timestep into a matrix in the workspace

```
>> about(result)
result [double] : 419x17 (56984 bytes)
```

which has one row per timestep, and each row contains the time followed by the state vector (elements 2–13) and the commanded rotor speeds ω_i (elements 14–17). To plot x and y versus time is

```
>> plot(result(:,1), result(:,2:3));
```

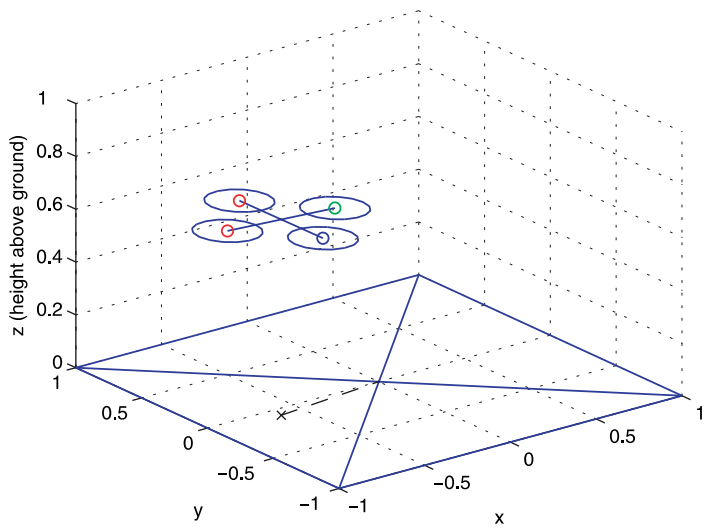

Fig. 4.18. One frame from the quadrotor simulation. The marker on the ground plane is a projection of the vehicle's centroid

4.4 Wrapping Up

In this chapter we have discussed general concepts about mobility, configuration space and task space. We created detailed models of two quite different robot platforms. We first discussed the car-like vehicle which is an exemplar of many ground robots. We developed a kinematic model which we used to develop a number of different controllers in order that the platform could perform useful tasks such as driving to a point, following a path or driving to a pose. We then discussed a simple flying vehicle, the quadrotor, and developed a dynamic model. We then implemented a number of nested control loops that allowed the quadrotor to fly a circuit. The nested control approach is described in more detail in Sect. 9.4.2.

The next chapters will discuss how to plan paths for robots through complex environments that contain obstacles and then how to determine the location of a robot.

Further Reading

Comprehensive modelling of mobile ground robots is provided in the book by Siegwart et al. (2011). In addition to the bicycle model covered here, it presents in depth discussion of a variety of wheel configurations with different combinations of driven wheels, steered wheels and passive casters. These topics are covered more succinctly in the Handbook of Robotics (Siciliano and Khatib 2008, § 17). Siegwart et al. also provide strong coverage of perception, localization and navigation which we will discuss in the coming chapters.

Ackermann's magazine can be found online at http://smithandgosling.wordpress.com/2009/12/02/ackermanns-repository-of-arts and the carriage steering mechanism is published in the March and April issues of 1818. King-Hele (2002) provides a comprehensive discussion about the prior work on steering geometry and Darwin's earlier invention.

Mobile ground robots are now a mature technology for transporting parts around manufacturing plants. The research frontier is now for vehicles that operate autonomously in outdoor environments (Siciliano and Khatib 2008, part F). Research into the automation of passenger cars has been ongoing since the 1980s but as yet there is no commercial offering – perhaps society is not yet ready for this technology or perhaps the legal complexities that might arise in the case of accidents is overwhelming.

The Navlab project at Carnegie-Mellon University started in 1984 and a series of autonomous vehicles, Navlabs, have been built and a large body of research has resulted. All vehicles make strong use of computer vision for navigation. In 1995 the supervised autonomous Navlab 5 made a 3 000-mile journey, dubbed "No Hands Across America" (Pomerleau and Jochem 1995, 1996). The vehicle steered itself 98% of the time largely by visual sensing of the white lines at the edge of the road.

In Europe, Ernst Dickmanns and his team at Bundeswehr Universität München demonstrated autononomous control of vehicles. In 1988 the VaMoRs system, a 5 tonne Mercedes-Benz van, could drive itself at speeds over 90 km h^{-1} (Dickmanns and Graefe 1988b; Dickmanns and Zapp 1987; Dickmanns 2007). The European Prometheus Project ran from 1987–1995 and in 1994 the robot vehicles VaMP and VITA-2 drove more than 1 000 km on a Paris multi-lane highway in standard heavy traffic at speeds up to 130 km h^{-1}. They demonstrated autonomous driving in free lanes, convoy driving, automatic tracking of other vehicles, and lane changes with autonomous passing of other cars. In 1995 an autonomous S-Class Mercedes-Benz made a 1 600 km trip from Munich to Copenhagen and back. On the German Autobahn speeds exceeded 175 km h^{-1} and the vehicle executed traffic manoeuvres such as overtaking. The mean time between human interventions was 9 km and it drove up to 158 km without any human intervention. The UK part of the project demonstrated autonomous driving of an XJ6 Jaguar with vision (Matthews et al. 1995) and radar-based sensing for lane

keeping and collision avoidance. More recently, in the USA a series of Grand Challenges were run for autonomous cars. The 2005 desert and 2007 urban challenges are comprehensively described in compilations of papers from the various teams in Buehler et al. (2007, 2010).

Flying robots and underwater are not yet discussed in standard robotics texts. The Handbook of Robotics (Siciliano and Khatib 2008) provides summaries of the state of the art of aerial and underwater robotics in chapters 41 and 43 respectively. The theory of helicopters with an emphasis on robotics is provided by Mettler (2003) but the definitive reference for helicopter dynamics is the very large book by Prouty (2002). The recent book by Antonelli (2006), now in second edition, provides comprehensive coverage of modelling and control of underwater robots.

Some of the earliest papers on quadrotor modelling and control are by Pounds, Mahony and colleagues (Hamel et al. 2002; Pounds et al. 2004, 2006). The thesis by Pounds (2007) presents comprehensive aerodynamic modelling of a quadrotor with a particular focus on blade flapping, a phenomena well known in conventional helicopters but mostly ignored for quadrotors. Quadrotors have been built at a number of laboratories and some are available commercially for hobbyists or for researchers. The Mikrokopter open-source project has designs for the airframe and propulsion system as well as control software and can be found at http://www.mikrokopter.de/ucwiki/en. The basic principle of the quadrotor is easily extended by adding more rotors and vehicles with 6, 8 and 16 rotors have been developed and this provides increasing payload capability and even redundancy to rotor failures.

Exercises

1. For a 4-wheel vehicle with $L = 2$ m and width between wheel centres of 1.5 m
   a) compute the difference in wheel steer angle for Ackerman steering around curves of radius 10, 50 and 100 m.
   b) If the vehicle is moving at 80 km h^{-1} compute the difference in back wheel rotation rates for curves of radius 10, 50 and 100 m.
2. Write an expression for turn rate in terms of the angular rotation rate of the two back wheels. Investigate the effect of errors in wheel radius and vehicle width.
3. Implement the $\ominus$ operator used in Sect. 4.2.1 and check against the code for `angdiff`.
4. Moving to a point (page 71) plot x, y and θ against time.
5. Pure pursuit example (page 74)
   a) Investigate what happens when the integral gain is zero. Now reduce the frequency of circular motion to 0.01 rev s^{-1} and see what happens.
   b) With integral set to zero, add a constant to the output of the controller. What should the value of the constant be?
   c) Modify the pure pursuit example so the robot follows a slalom course.
   d) Modify the pure pursuit example to follow a target moving back and forth along a line.
6. Moving to a pose (page 75)
   a) Repeat the example with a different initial orientation.
   b) Implement a parallel parking manoeuvre. Is the resulting path practical?
7. Use the MATLAB® GUI interface to make a simple steering wheel and velocity control, use this to create a very simple driving simulator. Alternatively interface a gaming steering wheel and peddle to MATLAB®.
8. Quadrotor (page 78)
   a) Experiment with different control gains. What happens if you reduce the damping gains to zero?
   b) Remove the gravity feedforward and experiment with high altitude-gain or a PI controller.
   c) Derive Eq. 4.13.

d) When the vehicle has non-zero roll and pitch angles, the magnitude of the vertical thrust is reduced and the vehicle will slowly descend. Add compensation to the vertical thrust to correct this.
e) Simulate the quadrotor flying inverted, that is, its z-axis is pointing upwards.
f) Program a ballistic motion. Have the quadrotor take off at 45 deg to horizontal then remove all thrust.
g) Program a smooth landing.
h) Program a barrel roll manoeuvre. Have the quadrotor fly horizontally in its x-direction and then increase the roll angle from 0 to 2π.
i) Program a flip manoeuvre. Have the quadrotor fly horizontally in its x-direction and then increase the pitch angle from 0 to 2π.
j) Add another four rotors.
k) Use the function `mstraj` to create a trajectory through ten via points $(X_i, Y_i, Z_i, \theta_y)$ and modify the controller of Fig. 4.17 for smooth pursuit of this trajectory.
l) Use the MATLAB® GUI interface to make a simple joystick control, and use this to create a very simple flying simulator. Alternatively interface a gaming joystick to MATLAB®.